

# PROPULSION ENERGY VERSUS FREE BALLAST SHIP CONCEPT PART TWO

I. NOVAC<sup>1</sup> C. GHEORGHE<sup>1</sup>

**Abstract:** *The ballast issue where ships are concerned has become a big problem lately, together with the invasive species transported between different areas of the ocean. Consequently, there are possibilities of replacing the classic ballast systems with another type to avoid “aliens invasion”. In the second part of this work we are introducing fundamental issues and the “free ballast ship” concept. Equally, we present the experimental research on the scale model.*

**Keywords:** *ship, ballast system, scale model, basin experiments, FBS ..*

## 1. Introduction

A doctoral thesis presented at the Maritime University of Constantza in feb. 2009, raised the matter of a new ballast system which permanently stays in touch with the sea. Two issues are in attention here

- i. the increase of ship's resistance and propulsion power demand due to openings in the ship's structure;
- ii. the advantages and disadvantages of permanent communication with the sea where the ballast system is concerned.

The current stage of this research project focuses on further hydrodynamic investigation of the BFS concept; both experimental and numerical.

The experimental investigation was performed by using a Bulk-Carrier

model and equally a General Cargo Ship. The initial investigation of the BFS concept proved the feasibility of the concept through a thorough examination of various design aspects. The effectiveness of the concept, in terms of eliminating the transport of foreign ballast water from ship operating in ballast condition, was also demonstrated by utilizing Computational Fluid Dynamics (CFD) software to simulate the flow in the double bottom ballast trunks of the vessel. Nevertheless, this initial investigation did not succeed in showing the full cost-effectiveness of the concept. The main reason was a significant fuel penalty that resulted from an increased power requirement found in the initial hydrodynamic testing of a non-optimized discharge configuration on an existing ship with a non-optimum propeller. Within the first

---

<sup>1</sup> Dept. of Naval and Mechanical Engineering, Maritime University of Constantza

part of the work we have gone into details with the issue's geometry and the basic concept of the new BFS .

Within the second part of the work we present the experiments consisting of detailed resistance and propulsion testing with and without the ballast trunk flow .

Finally , the third part , will present the CFD . The numerical investigation was performed CFD software, namely : FLUENT 6.0 .

**Note:** the numbering from the first part is to be continued .

### 3.3 Resistance Tests

*Experimental Test Plan* Table 3.3

Test speed	Ship speed (knots)	Model speed (m/s)	Froude number
1	14.50	1.210	0.173
2	15.50	1.295	0.185
3	16.50	1.378	0.197

The experimental test plan for both the resistance and propulsion tests is shown in Table 3.3. It was decided to test a range of speeds spanning a typical ballast condition operating range of bulk carriers of this size. The speed of 15.5 knots is considered as the designed ballast speed for purposes of flow scaling.

The resistance of the Ballast-Free bulk carrier model was measured and then extrapolated to full scale using the ITTC recommended method (ITTC 1978). The results for the full scale resistance and effective power are presented in Figs. 3.7 and 3.8, respectively.

For all testing conditions, the results are reported at a standard temperature of 15°C. Prior to the resistance tests, a static calibration test of the load cell was performed. Additional resistance tests were performed at low speeds to derive the form factor used in the extrapolation procedure. Errors related to the static calibration and the form factor derivation were considered as sources of bias error. Four different measurements were obtained at each speed shown in Table 3.3 in order to minimize the precision error.

The total uncertainty is calculated as the root sum square of the total bias error and the total precision error. The error bands shown in Figs. 3.7 and 3.8 correspond to the computed uncertainty values, assuming a 95% level of confidence.

The water discharge at the stern has a negative effect on ship resistance in both cases, even though the discharge at Station 17 seems to exacerbate the resistance increase.

Even though the resistance curves plotted in Fig. 3.7 show an increase in the average values, the difference with respect to the baseline case is not statistically significant as seen by the overlapping error bands.

### 3.4 Propulsion Tests

The resistance tests were followed by a series of propulsion tests using the MHL stock model propeller No. 23. The No. 23 stock propeller was the available propeller providing the highest propulsive efficiency and, at the same time, satisfying the hull clearance requirements, assuming a full-scale propeller diameter of 6.0 m.

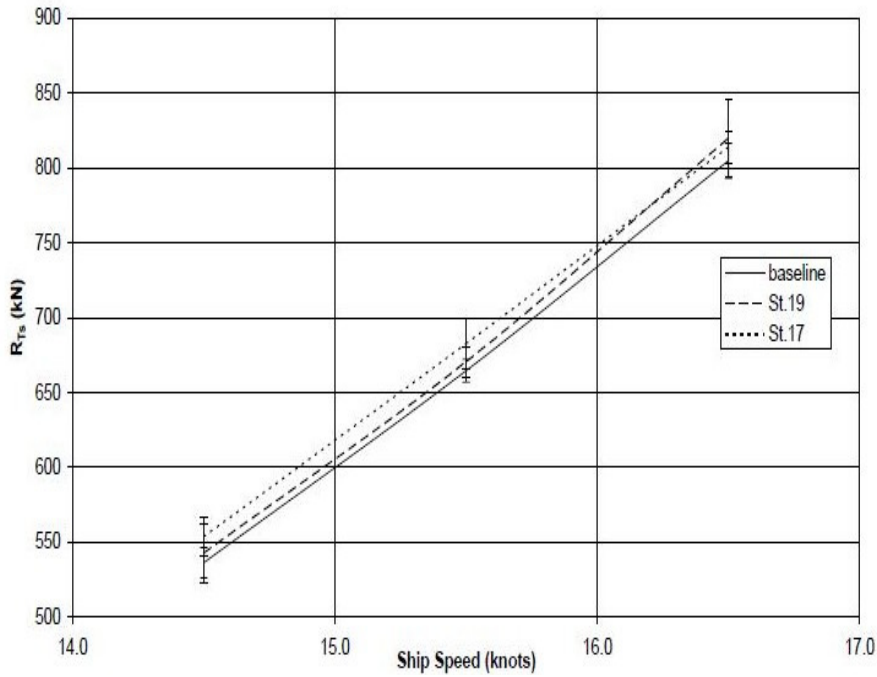


Figure 3.7 Ballast-Free Bulk Carrier Total Resistance

The propeller characteristics for the No. 23 model propeller are shown in Table 3.4. The non-dimensional thrust and torque coefficients plotted versus the coefficient of advance ( $K_t$ ,  $K_q - J$ ) of the No. 23 model propeller are shown in Fig. 3.9. The thrust and torque measurements at the self-

propulsion condition at each speed were analyzed using the ITTC-recommended method (ITTC 1978). The calculated required delivered power is shown in Fig. 3.10. An uncertainty analysis was also performed for the propulsion test results giving the error bands shown.

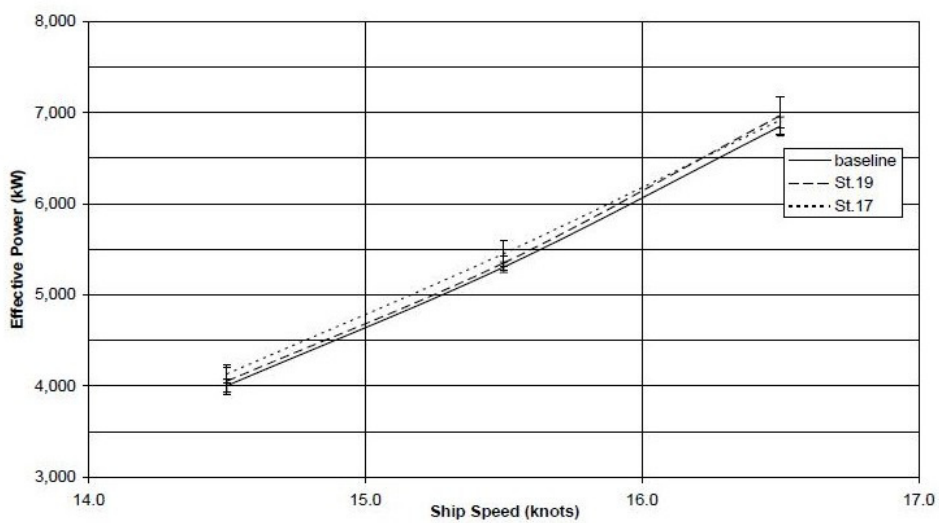


Fig. 3.8 Ballast-Free Bulk Carrier Total Effective Power

Characteristics of the MHL No. 23 Stock Propeller Table 3.4

Number of blades	4
Diameter $D_p$ (m)	0.158
Hub diameter (m)	0.031
Pitch-diameter ratio $P/D_p$	1.08
Expanded area ratio $A_e/A_o$	0.55

The propulsion test results depicted in Fig. 3.10 show a noteworthy reduction in the powering requirements caused by the water discharge at the stern. At a ballast condition speed of 15.5 knots, the reduction in the required delivered power is 7.3% for the discharge close to Station 17 and 2.1% for the discharge close to Station 19. Note that this is compared with a required delivered power increase of 7.4% observed in the initial investigation with the modified LASH vessel and the initial discharge configuration. A physical interpretation of this outcome

cannot be fully explained without a detailed analysis of the change in the effective wake entering the propeller with the trunk discharge and its interaction with the detailed propeller design. In the current phase of the project, a qualitative analysis of the results was attempted by utilizing CFD and analyzing the hull nominal wake. This analysis is presented in the next section. An additional advantage of fitting the preferred discharge location near Station 17, at least from an engineroom arrangements perspective, is that the ballast trunks would not have to be carried through the engineroom.

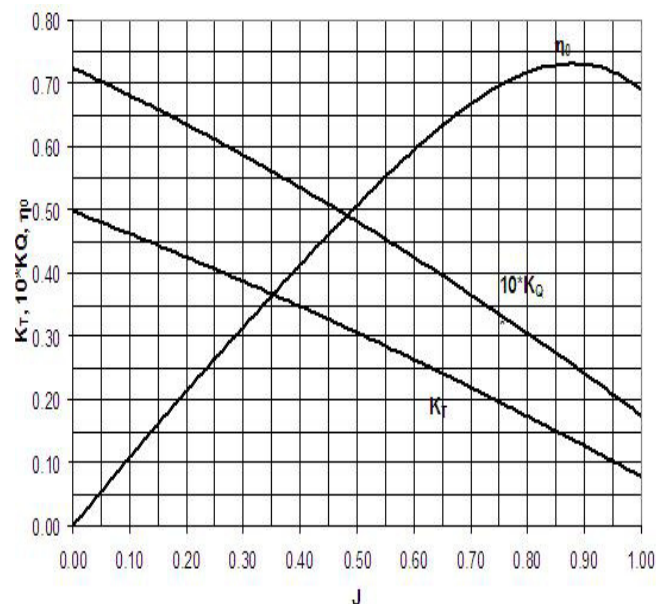


Figure 3.9. Propeller Coefficients vs. Advance Coefficient

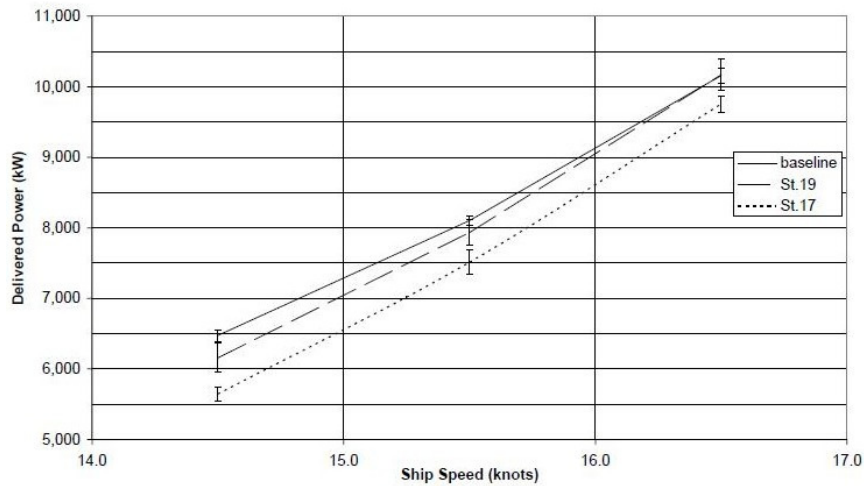


Fig. 3.10. Ballast-Free Bulk Carrier Required Delivered Power

### 3.5 Propeller Efficiency

Because a stock propeller was used in the experimental investigation, it was unclear to what extent the propulsion power reduction found would actually be realized if an optimum propeller design had been used on the model. The stock propeller utilized in the propulsion tests has characteristics quite similar to those of the standard Wageningen B-Screw Series B4-55 propeller (van Lammeren et al. 1969).

Therefore, an attempt was made to find the optimum, in terms of

efficiency, standard B-Screw Series propeller and compare its performance with the stock propeller utilized. In this manner, the margin of efficiency improvement of the stock propeller used could be estimated. This could help clarify whether the utilization of an optimum propeller could have benefited as much as the stock propeller from the ballast trunk discharge effect. The results of the analysis for the optimum B-Screw Series propeller the ballast speed of 15.5 knots are shown in Table 3.5.

Analysis for the optimum B-Screw Series propeller

Table 3.5

$P/D_p$	$\eta_B$	$n$ (rpm)	$\sigma$	$\tau_c$	Back Cavitation (%)	$J$
0.5	0.510	137	0.368	0.100	0.5	0.321
0.6	0.543	121	0.473	0.131	1.0	0.364
0.7	0.555	108	0.582	0.166	1.5	0.405
0.77	0.558	102	0.659	0.191	2.2	0.433
0.8	0.556	99	0.693	0.202	2.5	0.444
0.9	0.551	92	0.804	0.241	3.5	0.480
1.0	0.541	86	0.915	0.282	4.5	0.513
1.08	0.532	81	1.023	0.324	5.5	0.545
1.2	0.517	77	1.128	0.368	6.5	0.574
1.3	0.506	73	1.231	0.413	7.5	0.601
1.4	0.497	70	1.330	0.460	8.5	0.627

The result in Table 3.5 show that a 4-bladed propeller with a pitch-diameter ratio of 0.77 provided the optimum efficiency  $\eta_B = 0.558$  with an acceptable extent (2.2%) of a back cavitation. A comparison of the efficiency of two

B-Screw propellers with the model stock propeller in the three test conditions (no ballast trunk flow or baseline and discharge at Stations 17 and 19) is shown in Table 3.6.

Propeller Efficiency  $\eta_B$

Table 3.6

MHL No.23 Propeller – baseline	0.556
MHL No.23 Propeller – Station 17	0.565
MHL No.23 Propeller – Station 19	0.558
B4-55 (P/D = 1.08, same as No. 23)	0.532
Optimum B4-55 (P/D = 0.77)	0.558

These results reveal that an improvement in propeller efficiency when operating behind the ship hull of about 4.9% (from 0.532 to 0.558) might be achieved by utilizing an optimum propeller. On the other hand, a different picture is observed when the ballast trunks are discharging at the stern. The propeller efficiency is slightly increased when discharging close to Station 19 and more significantly increased (1.6%) when discharging close to Station 17. Therefore, it can be argued that an optimum propeller will probably not benefit quite as

much, in terms of propeller efficiency, as the stock propeller utilized.

However, a significant part of the overall propulsive efficiency improvement can be attributed to the increase of the hull efficiency, as shown in Table 3.7. Thus, it appears that most of the required power improvement (actually a small apparent resistance increase and a 7.3% delivered power reduction) observed would still be realized when an optimum propeller were used.

Hull Efficiency and Propulsive Efficiency

Table 3.7

	Hull Efficiency $\eta_H$	Propulsive Efficiency, $\eta_P = \eta_B * \eta_H$
MHL No.23 Propeller – baseline	1.194	0.664
MHL No.23 Propeller – Station 17	1.286	0.727
MHL No.23 Propeller – Station 19	1.214	0.677

## References

1. Duvigneau, R., Visonneau, M. et al.: *On the Role Played by Turbulence Closures in Hull Shape Optimization at Model and Full Scale*. In: 24th Symposium on Naval Hydrodynamics, Fukuoka, Japan, August 8-13, 2002.
2. Dyne, G.: *The Principles of Propulsion Optimization*, In: *Transactions RINA*, 137, 1995, p. 189-208.
3. *FLUENT 6.3 User's Manual*, Fluent Inc., Lebanon, NH, 2006.
4. *International Convention for the Control and Management of Ships' Ballast Water & Sediments*, Diplomatic Conference, February, London.
5. *ITTC 15th International Towing Tank Conference*, 3-10 September 1978, The Hague, The Netherlands", Netherlands Ship Model Basin, Wageningen.
6. Novac, I.: *Maritime Technology*. In: *Masteral Course*, Constanta, UMC 2008.
7. Novac, I.: *Research Methodology*. In: *Masteral Course*, Constanta, UMC 2008.
8. Popa, D.S. CLC: *Noi concepte de proiectare navala privind prevenirea poluarii cu apa de ballast*. In Ph.D. Thesis, Constanta, UMC, Romania 2009.